Evaluation of midlatitude cloud properties in a weather and a climate model: Dependence on dynamic regime and spatial resolution

George Tselioudis

NASA/Goddard Institute for Space Studies and Columbia University Department of Applied Physics, New York, New York, USA

Christian Jakob[1]

European Centre for Medium-Range Weather Forecasts, Reading, United Kingdom

[1] In this study, the midlatitude cloud fields produced by a climate (GISS) and a weather (ECMWF) model are evaluated against satellite observations. Monthly ensembles of model cloud property distributions for the four seasons are compared with similar ensembles from satellite retrievals. The weather model is run in both forecast and "climate" mode in order to evaluate the importance of the exact representation of the atmospheric conditions in these ensemble comparisons. The weather and climate models are evaluated at different resolutions that cover the range used in today's climate and weather prediction simulations. Cloud property evaluations are separated into broadly defined dynamic regimes that cover the range of large-scale midlatitude motions. Quantitative evaluation tables are produced that rank the performance of the different model versions used in the study. The evaluation analysis reveals several common features between the two models. Those are the overestimation of cloud optical depth in all dynamic regimes, the underestimation of cloud cover in the large-scale descent regime and the underestimation of cloud top height in the large-scale descent regime. It is also shown that, in the radiative balance calculations, the models compensate for the overestimation of cloud optical depth through the underprediction of cloud cover. The comparison of the forecast and "climate" runs of the ECMWF model shows remarkably similar statistical properties of the clouds in the two runs. The analysis of runs with different resolutions reveals large improvement when going from a $4° \times 5°$ 9-layer to a $2° \times 2.5°$ 32-layer run with the GISS GCM, much of which is caused by the increase in vertical resolution. A comparison of a T42 and a T106 run of the same vertical resolution with the ECMWF GCM does not show considerable differences between the two model versions.   *INDEX TERMS:* 0320 Atmospheric Composition and Structure: Cloud physics and chemistry; 3337 Meteorology and Atmospheric Dynamics: Numerical modeling and data assimilation; 3319 Meteorology and Atmospheric Dynamics: General circulation; 3359 Meteorology and Atmospheric Dynamics: Radiative processes; 3360 Meteorology and Atmospheric Dynamics: Remote sensing; *KEYWORDS:* Clouds, model, evaluation, midlatitudes, weather, climate

1. Introduction

[2] In the midlatitude regions, the cycling of water by cloud formation and precipitation processes is governed to a large extent by the large-scale atmospheric dynamics. Optically thick, heavily precipitating clouds tend to occur in low pressure/rising air regimes, while drizzling or nonprecipitat-

ing low-cloud decks are found in high pressure/sinking air regimes [*Lau and Crane*, 1995, 1997; *Tselioudis et al.*, 2000]. The differences in cloud type distributions between midlatitude dynamic regimes produce top-of-the-atmosphere differences in net absorbed radiation that can reach magnitudes of 50W/m^2 and that vary greatly with seasonal insolation [*Tselioudis et al.*, 2000; *Weaver and Ramanathan*, 1996, 1997].

[3] Climate model simulations produce large errors in both long- and short-wave midlatitude radiative budgets, and the description of clouds has often been blamed for those errors [e.g., *Hahmann et al.*, 1995; *Del Genio et al.*,

[1]Now at Bureau of Meteorology Research Centre, Melbourne, Australia.

1996]. A case in point is the GISS GCM, whose latitudinal patterns of cloud and radiation errors are characteristic of those found in a number of GCMs as shown in the Atmospheric Model Intercomparison Project [*Gleckler et al.*, 1995].

[4] The GISS GCM overestimates middle and high latitude absorbed shortwave radiation and underpredicts longwave cloud forcing relative to ERBE at these latitudes [*Del Genio et al.*, 1996]. The peak model differences with observations occur along the main storm tracks off the east coasts of North America and Asia. The consequences of an inadequate simulation of midlatitude cloud properties by climate models are numerous. They include the incorrect simulation of hydrologic and radiative climate feedbacks with large consequences in the prediction of changes in drought severity and frequency [*Hansen et al.*, 1989] and changes in the diurnal temperature range [*Dai et al.*, 1997], as well as potentially large errors in the calculation of ocean heat transports [*Gleckler et al.*, 1995] and their changes with climate.

[5] It is, therefore, crucial to evaluate the ability of climate models to simulate correctly the cloud type distributions in the midlatitude regions. The GEWEX Cloud System Study (GCSS) Working Group on midlatitude layered clouds was formed with the intention to improve the representation of such clouds in climate models. The large dependence of midlatitude cloud properties on atmospheric dynamics and the potential for cloud feedbacks resulting from dynamical changes [*Tselioudis et al.*, 2000] makes it necessary to evaluate model simulations of midlatitude clouds in relation to dynamic processes. In recent years, a few studies have examined specific aspects of the performance of weather and climate models in simulating midlatitude cloud and radiation fields. *Klein and Jakob* [1999] used the ECMWF numerical weather prediction (NWP) model to compare cloud structures in forecasts of intense North Atlantic cyclones to satellite and surface observations of the same cyclones from studies by *Lau and Crane* [1995, 1997]. They found that while the model simulated correctly the main cloud structures and their location with respect to the low-pressure center, errors occurred in the simulation of the cloud optical properties that were specific to the different sectors of the storm. *Ryan et al.* [2000] found that simulations of a Southern Hemisphere storm by limited area models had much larger cloud errors in the weakly forced, beginning stages rather than the strongly forced, mature stages of the storm. *Norris and Weaver* [2001] compared North Pacific cloud and radiation fields simulated by the NCAR climate model to satellite observations and found that the model overpredicts cloud forcing in large-scale ascent regimes and underpredicts cloud forcing in large-scale descent regimes. *Webb et al.* [2001] compared cloud and radiation properties in selected regions around the globe to simulations by three climate models. In the Northern Pacific storm track, they found that the majority of the models underpredict both the shortwave and the longwave cloud radiative forcing.

[6] The studies mentioned above concentrate on the radiative effects of midlatitude clouds and provide information on model cloud property deficiencies that are specific to particular regions or storm types. They do not, however,

provide a detailed evaluation of midlatitude model cloud properties that includes land and ocean regions, resolves the seasonal cycle, and examines changes in model performance with resolution for the whole range of midlatitude dynamic regimes. This is attempted in the present study, where the midlatitude cloud fields produced by a climate and a weather model are evaluated against satellite observations. Monthly ensembles of model cloud property distributions for the four seasons are compared with similar ensembles from satellite retrievals. The weather model is run in both forecast and "climate" mode in order to evaluate the importance of the exact representation of the atmospheric conditions in these ensemble comparisons. The weather and climate models are evaluated at different resolutions that cover the range used in today's climate and weather prediction simulations. Cloud property evaluations are separated into broadly defined dynamic regimes that cover the range of large-scale midlatitude motions, in order to gain some insight into the processes responsible for potential cloud property deficiencies. Quantitative evaluation tables are produced that rank the performance of the different model versions used in the study. Section 2 describes the model and observational data sets used in the study, and discusses the analysis methods applied to the data. The results of the model evaluations are presented in section 3, while section 4 includes a discussion on the main issues presented in the paper.

2. Data Sets and Analysis Methods
2.1. The ECMWF Reanalysis/Definition of Dynamic Regimes

[7] Defining dynamic regimes for use in the subsequent satellite cloud data analysis requires knowledge about parameters characterizing the regimes, such as surface pressure, vertical velocity, and vorticity on a global scale. The only sources of such information are global analyses as produced by NWP centers several times a day. Here we use the ECMWF reanalysis (ERA) data set [*Gibson et al.*, 1997]. The aim when defining a dynamic regime is to use a simple criterion that nevertheless captures the difference in the prevailing cloud regimes in the region of interest. *Tselioudis et al.* [2000] used surface pressure anomalies to distinguish different cloud regimes over the Northern Hemisphere midlatitude regions. The idea was to capture cloud and radiation differences between the different sectors of a baroclinic storm. *Lau and Crane* [1995] showed that cloud type differences in baroclinic storms are captured better through the use of the large-scale vertical velocity field. For that reason this study uses negative and positive values of vertical velocity at 500hPa to distinguish two regimes, one of large-scale ascent and one of large-scale descent. ERA analyses of the vertical velocity at 2.5 degrees resolution are used every 12 hours for the months of January, April, July and October 1992 to define the two regimes for the Northern midlatitudes ($30°-60°N$). It must be noted that when parts of this analysis were repeated using the NCEP reanalysis products no significant differences from the results presented here were found. Also, several months of data from years other than 1992 were examined and, despite small quantitative differences, the character of the results presented in this study remained the same.

2.2. The ISCCP Data Set/Construction of Satellite Cloud Property Composites

[8] The cloud data set analyzed in this study is produced by the International Satellite Cloud Climatology Project (ISCCP) [*Rossow and Schiffer*, 1999; *Rossow et al.*, 1996]. The data set contains detailed information on the distribution of cloud radiative properties and their diurnal and seasonal variations, as well as information on the vertical distribution of temperature and humidity in the troposphere. The data are based on observations from the suite of operational weather satellites. The revised (D1) version of the data set used in this study has a spatial resolution of 280 km (2.5 degrees at the equator) and a temporal resolution of three hours. For each map grid-box, the number of cloudy pixels (approximately 5 km in size) that belong to each of seven pressure levels and six optical thickness ranges is reported. In other words, all cloudy pixels in a grid-box are placed in one of 42 cloud optical thickness-cloud top pressure types. Figure 1 shows the six optical thickness ranges and the vertical resolution of the seven cloud top pressures, together with radiometric definitions of nine cloud types. A total of fifteen cloud types are included in the data set, since warm low and middle level clouds are defined and treated as liquid clouds and cold low and middle level clouds are defined and treated as ice clouds.

[9] After defining the upward and downward motion regimes from the ECMWF reanalysis data, the ISCCP retrievals of cloud optical thickness (TAU) and cloud top pressure (CTP) are used to construct TAU-CTP frequency histograms for each corresponding vertical velocity regime. The histograms are constructed by dividing the forty-two TAU-CTP cloud types in each 12-hour observation with the total cloud cover in the grid box and then calculating for the whole month the percentage of occurrences in each dynamic regime of a cloud of a certain TAU-CTP type. The histograms, then, reveal the cloud types that are dominant in large-scale ascent and large-scale descent regimes. Note that, since cloud optical thickness values are available only during daytime, not all 12-hourly observations in a month are used to construct the TAU-CTP histograms, and that liquid and ice clouds are merged together in each cloud type. From the histograms, the total cloud cover in each regime is calculated by adding the cover of all forty-two TAU-CTP types. The use of cloud type histograms for different dynamic regimes was introduced by *Tselioudis et al.* [2000] and was used in other recent studies [e.g., *Norris and Weaver*, 2001].

2.3. The ECMWF and GISS Models/Construction of Model Cloud Property Composites

[10] The main model information to be compared to the ISCCP observations is the TAU-CTP histograms. Constructing this type of histogram from a GCM simulation is far from trivial and several methods have been proposed. Here a method to subdivide a model grid-box into smaller boxes (equivalent to satellite pixels in the data) and to simulate the "top-down" view of cloud properties by the satellite is adopted. The method was originally developed by *Jakob and Klein* [1999] and extended to simulate ISCCP data by *Klein and Jakob* [1999]. Starting from the model simulated cloud cover and cloud condensate content at each model layer, each gridbox is split into 100 smaller boxes. The cloud condensate is distributed into these subboxes in
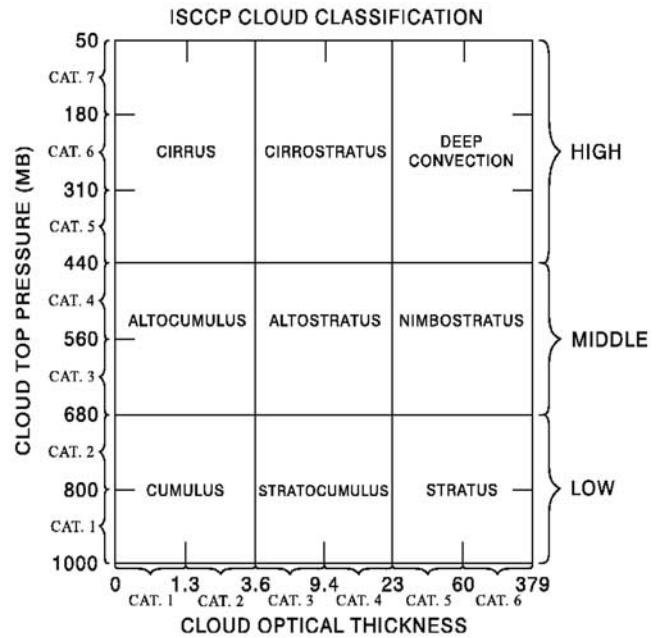
Figure 1. Definitions of cloud optical thickness and cloud top pressure categories, together with radiometric definitions of nine cloud types, from the ISCCP D1 data set.

each model layer using the model's cloud overlap assumption [*Morcrette and Jakob*, 2000]. Then for each subbox cloud top pressure and cloud optical thickness are calculated and a TAU-CTP histogram is constructed for each model gridbox from the 100 "pixels" available. For more details the reader is referred to the appendix in *Klein and Jakob* [1999].

[11] The method described above was applied to output from simulations with the ECMWF weather model [*Gregory et al.*, 2000], and the GISS climate model [*Hansen et al.*, 1983; *Del Genio et al.*, 1996]. The ECMWF model is run in both forecast and "climate" mode in order to evaluate the importance of the exact representation of the atmospheric conditions in these cloud ensemble comparisons. The two models are evaluated at different spatial resolutions that cover the range used in today's climate and weather prediction simulations Details of the different runs that were used to construct the cloud property composites are presented in the next section of the paper.

3. Results

[12] The cloud statistics that will be used in the model evaluation analysis are taken over periods of one month, in the 30°–60°N region, separately for land and ocean and for the upward and downward vertical velocity regimes. Results for the month of April will be shown first and the model clouds will be compared to ISCCP observations for April 1992. The use of a weather model in this evaluation study allows us to examine differences between cloud statistics produced by a forecast model run using the dynamical conditions of April 92 and those produced by a climatological April simulation. To do that, we construct cloud property composites from 12-hour ECMWF forecasts with a

T106 (~1°) 31-layer model for April 92 (forecast run) and compare them with similar composites from a one-month "free" run of the same model initialized with April initial conditions ("climate" run). The comparison is shown in the four-paneled Figure 2, where the left two panels represent clouds over ocean and the right two panels clouds over land, while the top two panels represent the large-scale ascent and the bottom two panels the large-scale descent regimes; on each panel the left column shows the climate run, the middle column the forecast run and the right column the difference between the two runs. Cloud optical thickness-cloud top pressure histograms are presented at the top of each column and tables with the cloud cover values in six broad cloud categories at the bottom. The total cloud cover is noted in parenthesis at the top of each cloud property histogram. It can be seen that, particularly over ocean, very small differences occur between the cloud distributions of the climate and forecast runs. As a rule, the forecast run has less cloud cover than the climate run, while over land the climate run makes higher and somewhat optically thicker clouds than the forecast run. It is not obvious why the different simulations behave in this manner. Clearly the different behavior of the short-range forecasts is caused by the ingestion of data during the data assimilation cycle. It may be that in the ECMWF data assimilation system the use of humidity data from satellite retrievals over the ocean tends to lead to a moistening of the atmosphere, while the use of moisture data from radiosonde measurements tends to lead to upper tropospheric drying over land.

[13] A comparison between the ECMWF T106 31-layer climate run for April and ISCCP cloud retrievals for April 1992 is presented in Figure 3. The format of the figure is the same as in Figure 2 with the only difference that here the ISCCP retrievals occupy the middle column of each panel. In the large-scale ascent regime (top panels), both the model and the observations show a wide variety of cloud types that include the high, optically thick clouds typically associated with storm events, but also contain high and midlevel thin clouds in the observations and midlevel thick clouds in the model simulation. The model predicts rather well the total cloud cover, as it puts it in the upper 80% range over ocean and in the lower 80% range over land. In the vertical domain, the model distributes the clouds somewhat different than the observations, overpredicting the amount of clouds with high tops and underpredicting the amount of clouds with low tops by approximately equal amounts. Finally, the model severely overpredicts the optical thickness of all clouds produced in the ascent regime. In the large-scale descent regime (bottom panels), both the model and the observations show a predominance of low clouds with some additional middle and high-level thin clouds present. The model underpredicts the total cloud cover in this regime by about 20% both over ocean and over land. This under-prediction is mostly due to a lack of midlevel thin clouds in the model simulation. The model also severely overpredicts the optical thickness of the low cloud deck in the large-scale descent regime. It is important to note here that the cloud type separation into vertical velocity regimes of the ISCCP data produces results similar to the cloud type separation into sea level pressure regimes [*Tselioudis et al.*, 2000]. The results of the two methods differ only in that the vertical velocity regime separation shows sharper contrasts between
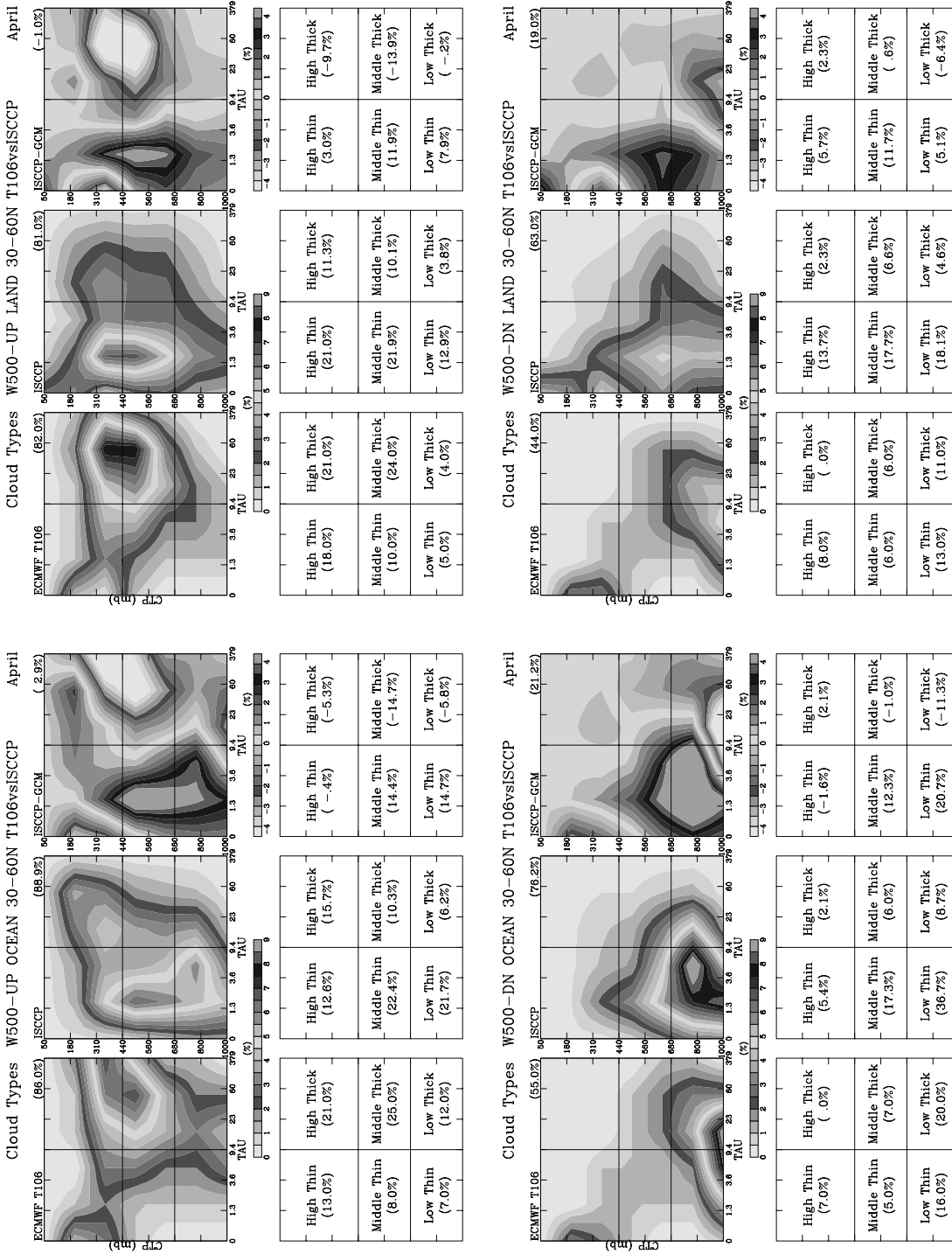
the height and optical thickness of the low and high cloud decks found in the downward/high-pressure and upward/low-pressure regimes. This implies that, to the extend that they can be used to separate the different sectors of a baroclinic storm, a number of different parameters can be used as the basis for dynamic regime separation of the midlatitude clouds. Guidance for the relations between cloud properties and midlatitude dynamic parameters is provided in *Lau and Crane* [1995].

[14] A comparison between a GISS 2° × 2.5° 32-layer climate run for April and ISCCP cloud retrievals for April 1992 is presented in Figure 4. In the large-scale ascent regime (top panels) the model underpredicts the total cloud cover by 10% over ocean and by 20% over land. This underprediction is mostly due to the small amounts of high clouds (both thin and thick over ocean and mostly thin over land) produced in the model simulation. As with the ECMWF simulation, the model overpredicts the optical thickness of almost all cloud types. In the large descent regime (bottom panels) the model underpredicts total cloud cover by 14% over ocean and by 22.5% over land. This is due to a lack of midlevel and high thin clouds in the model simulation. The model also overpredicts the optical depth of the low cloud deck mainly over land areas, and under-predicts the top height of the low clouds in this regime. The underprediction by global models of midlevel thin clouds is also found in the analysis of North Pacific cloudiness of *Webb et al.* [2001]. Our results show that this underprediction happens primarily in the large-scale descent regime where models tend to produce low cloud decks that are mostly confined to the boundary layer.

[15] To examine the effects of changing resolution on the simulation of midlatitude cloud properties, the same analysis for the month of April was performed on output from a 4° × 5° 9-layer version of the GISS GCM and a T42 (~2.5°) 31-layer version of the ECMWF GCM. A quantitative comparison between the cloud properties of the four model versions and the ISCCP retrievals is presented in Table 1. The table presents the difference between the model-simulated and satellite-retrieved values of three cloud properties (cloud cover-ΔCLC, albedo of the cloud-$\Delta\alpha$cl and of the scene (i.e., cloud + clear sky)- $\Delta\alpha$sc, and cloud top pressure-ΔCTP), and the correlation coefficient R between the simulated and the observed cloud property patterns. Those four quantities are presented separately for the upward and downward vertical velocity regimes and for clouds over land and ocean. Starting with the GISS GCM, the main differences with the ISCCP observations are the lower cloud cover, higher cloud albedo, and lower cloud top height (higher cloud top pressure) of the model in all regimes. It is interesting to note that the model to some degree compensates for the lower cloud cover with the higher cloud albedo, producing scene albedo (the albedo of the cloudy and clear sky together) differences with the observations that are much smaller than the cloud albedo differences themselves. In terms of the effects on model performance of resolution changes, the increase in both horizontal and vertical resolution of the model improves the agreement with the satellite retrievals in pretty much every cloud parameter and dynamic regime. The higher resolution model produces higher cloud amounts, lower optical depths, and higher cloud tops than the lower resolution
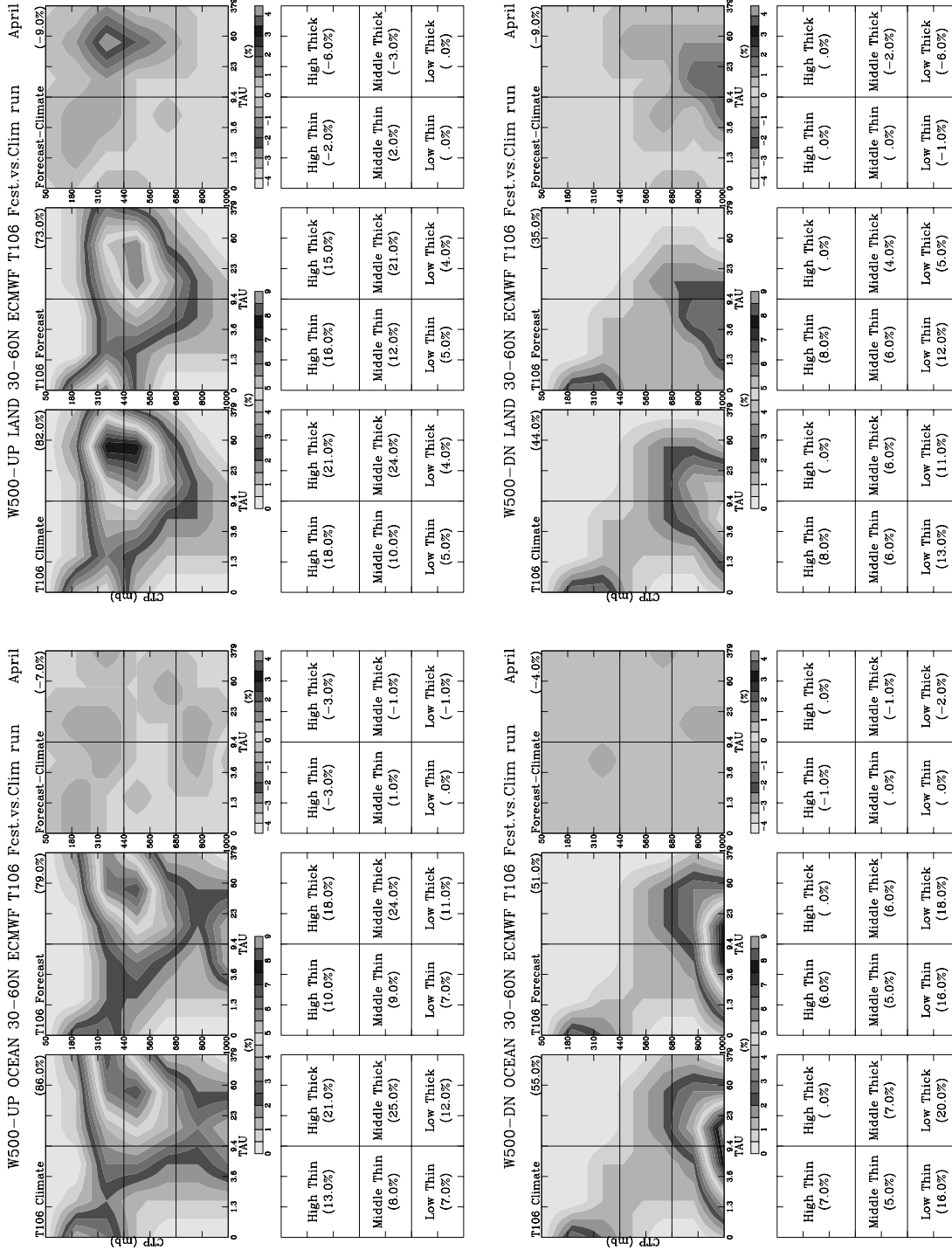
Figure 2. Top two panels represent the large-scale ascent and the bottom two panels the large-scale descent regime, and the left two panels show clouds over ocean and the right two panels clouds over land. Each panel includes cloud optical thickness-cloud top pressure histograms (top row) and tables with cloud cover values in six broad cloud categories (bottom row), for the ECMWF T106 climate run (left column) forecast run (middle column) and the difference between the two (right column). The total cloud cover is noted in parenthesis at the top of each cloud property histogram. See color version of this figure at back of this issue.

Figure 3. Top two panels represent the large-scale ascent and the bottom two panels the large-scale descent regime, and the left two panels show clouds over ocean and the right two panels clouds over land. Each panel includes cloud optical thickness-cloud top pressure histograms (top row) and tables with cloud cover values in six broad cloud categories (bottom row), for the ECMWF T106 climate run (left column) ISCCP retrievals (middle column) and the difference between the two (right column). The total cloud cover is noted in parenthesis at the top of each cloud property histogram. See color version of this figure at back of this issue.
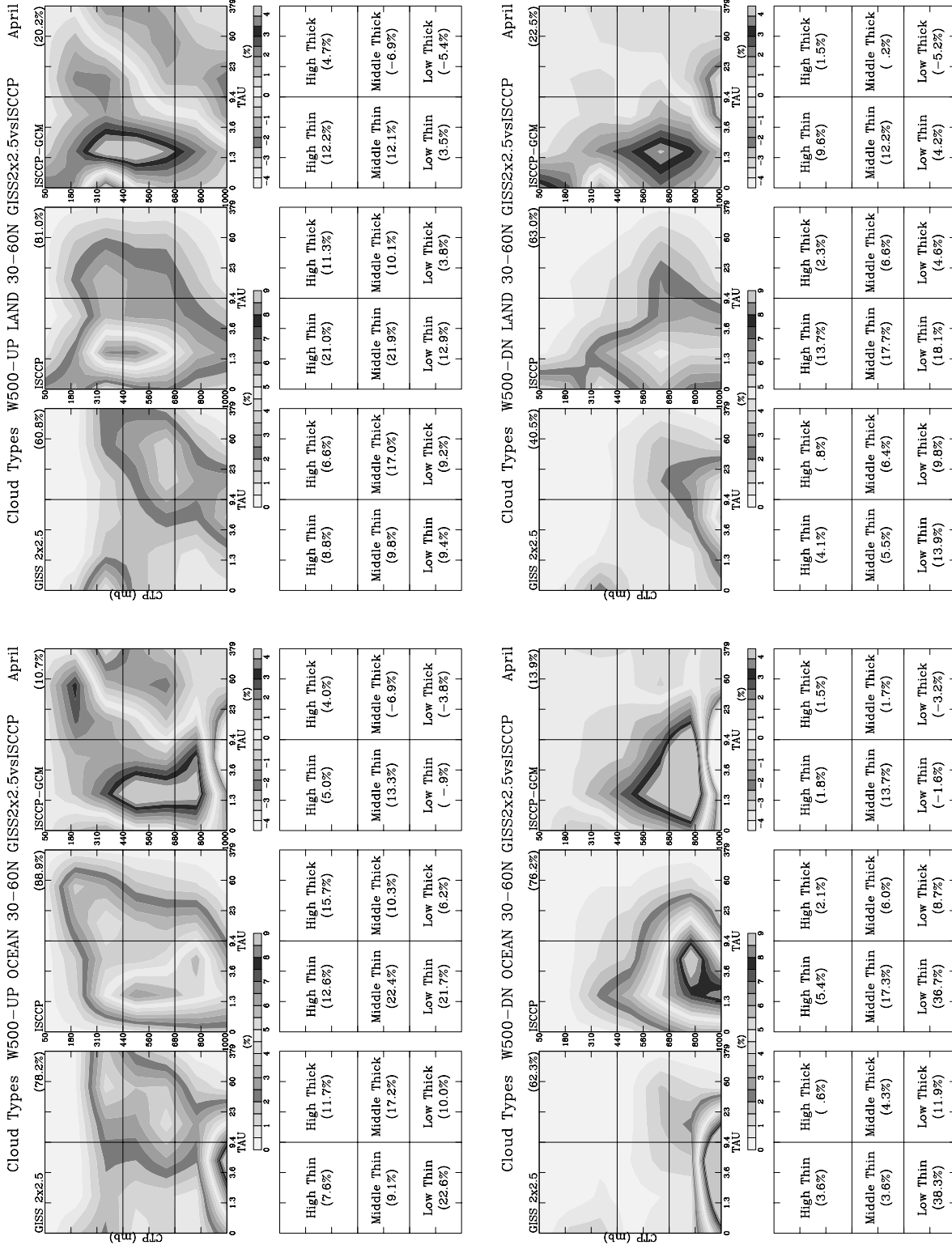
Figure 4. As in Figure 3 for the GISS $2° \times 2.5°$ 32-layer model. See color version of this figure at back of this issue.

Table 1. Satellite-Model Differences of Cloud Cover (ΔCLC), Cloud Albedo ($\Delta\alpha$cl), Scene Albedo ($\Delta\alpha$sc), and Cloud Top Pressure (ΔCTP), and the Satellite-Model Cloud Pattern Correlation Coefficient (R)[a]

	ISCCP - GCM	GISS 4 × 5 × 9	GISS 2 × 2.5 × 32	ECMWF T42	ECMWF T106
	ΔCLC (%)	19.7	10.7	−3.1	2.9
W-UP	R	0.06	0.3	0.14	0.12
OCN	$\Delta\alpha$cl ($\Delta\alpha$sc) (%)	−15 (−2.1)	−7.5 (−1.4)	−18.3 (−18.2)	−17 (−13.4)
	ΔCTP (mb)	−118	−80.7	44.3	31.3
	ΔCLC (%)	28	20.2	−3	−1
W-UP	R	0.2	0.16	0.37	0.31
LAND	$\Delta\alpha$cl ($\Delta\alpha$sc) (%)	−16.8 (1.62)	−13.3 (−0.5)	−9.2 (−8.9)	−16.4 (−13.8)
	ΔCTP (mb)	−92.6	−87.9	−26	31.3
	ΔCLC (%)	35.8	13.9	21.2	21.2
W-DN	R	0.22	0.48	0.5	0.38
OCN	$\Delta\alpha$cl ($\Delta\alpha$sc) (%)	−15 (6.5)	−2.1 (3.6)	−10.7 (1.5)	−12.3 (0.7)
	ΔCTP (mb)	−152	−117	−37	−33
	ΔCLC (%)	35.5	22.5	13	19
W-DN	R	0.16	0.34	0.55	0.41
LND	$\Delta\alpha$cl ($\Delta\alpha$sc) (%)	−19.3 (5.8)	−12.2 (2.1)	−1.6 (3.2)	−10.3 (1.4)
	ΔCTP (mb)	−136.4	−126.2	−147	−90.2

[a]The results are for upward and downward vertical velocity regimes and for clouds over land and ocean for the month of April. The models shown are the GISS 4° × 5° 9-layer, GISS 2° × 2.5° 32-layer, ECMWF T42 31-layer, and ECMWF T106 31-layer.

one, bringing the model midlatitude cloud properties closer to the observed ones. As a result, the cloud pattern correlation coefficients improve with the resolution increase in almost all dynamic regimes. A subsequent analysis of a 4° × 5° 53-layer version of the GISS GCM (results not shown here) showed large increases in midlatitude cloud top height and smaller increases in cloud cover compared to the 4° × 5° 9-layer version, but very small changes in cloud optical depth. This implies that the improvement with resolution in midlatitude cloud heights and covers in the GISS GCM may be coming mainly through increases in vertical resolution while the improvement in cloud optical depth may be coming mainly through increases in horizontal resolution.

[16] Both the T106 and T42 versions of the ECMWF model (Table 1) show cloud cover amounts that are similar to the observed ones in the large-scale ascent regime, but are much smaller than the observed in the large-scale descent regime. Cloud albedo values are higher that the retrieved ones in all regimes; in the large-scale descent regime the lower cloud covers compensate for the higher optical depths producing scene albedo differences with the observations that are smaller than the cloud albedo differences. Cloud top pressure values are in relatively good agreement with the

retrieved ones in the large-scale ascent regime but are larger than the retrieved ones in the large-scale descent regime, particularly over land regions. A comparison of the two ECMWF runs does not show any obvious advantages of the run with the higher horizontal resolution. Overall, the T42 run has higher pattern correlation coefficients implying that it simulates better the pattern of cloud optical property distribution in the different regimes, while the T106 run produces cloud top pressures that are in somewhat better agreement with the satellite retrievals.

[17] The model cloud evaluation analysis detailed above was performed for the four canonical months of the year (January, April, July, and October) in order to examine potential seasonal characteristics of the model-satellite differences. The model-satellite differences for the GISS 2° × 2.5° 32-layer and the ECMWF T106 31-layer runs for January and July are summarized in Tables 2 and 3 respectively. Overall, the conclusions that were derived from the analysis of the April results remain valid when data from the other months are analyzed. As a rule, the model underprediction of cloud cover in the large-scale descent regime is smaller in January than in any other month and it is largest in July in continental locations. This difference between seasons might be caused by an improper

Table 2. As in but for January and for the GISS 2° × 2.5° 32-Layer and ECMWF T106 31-Layer Models

	ISCCP - GCM	GISS 2 × 2.5 × 32	ECMWF T106
	ΔCLC (%)	3.1	0.8
W-UP	R	0.21	−0.07
OCN	$\Delta\alpha$cl ($\Delta\alpha$sc) (%)	−9.6 (−6.8)	−21.2 (−17.9)
	ΔCTP (mb)	−113	17
	ΔCLC (%)	10.9	−7.1
W-UP	R	0.31	0.69
LAND	$\Delta\alpha$cl ($\Delta\alpha$sc) (%)	−4.15 (2.13)	−0.3 (−3.3)
	ΔCTP (mb)	−139	−36
	ΔCLC (%)	3.5	16.6
W-DN	R	0.49	0.4
OCN	$\Delta\alpha$cl ($\Delta\alpha$sc) (%)	−5.8 (−3.1)	−14.7 (−3.4)
	ΔCTP (mb)	−129	−20
	ΔCLC (%)	5.2	13.9
W-DN	R	0.48	0.41
LND	$\Delta\alpha$cl ($\Delta\alpha$sc) (%)	−2 (1)	10.5 (10.3)
	ΔCTP (mb)	−119	−126

Table 3. As in but for July and for the GISS 2° × 2.5° 32-Layer and ECMWF T106 31-Layer Models

	ISCCP - GCM	GISS 2 × 2.5 × 32	ECMWF T106
	ΔCLC (%)	5.6	1.4
W-UP	R	0.5	0.17
OCN	$\Delta\alpha$cl ($\Delta\alpha$sc) (%)	−2.66 (0.46)	−18.4 (−14.3)
	ΔCTP (mb)	−81.5	41.7
	ΔCLC (%)	19.8	14.9
W-UP	R	0.14	0.12
LAND	$\Delta\alpha$cl ($\Delta\alpha$sc) (%)	−15 (−0.9)	−24.3 (−9)
	ΔCTP (mb)	−86.5	68.2
	ΔCLC (%)	8.4	14.6
W-DN	R	0.59	0.45
OCN	$\Delta\alpha$cl ($\Delta\alpha$sc) (%)	3 (5.2)	−10.3 (0.05)
	ΔCTP (mb)	−130.6	−85
	ΔCLC (%)	24.1	27.1
W-DN	R	0.23	0.18
LND	$\Delta\alpha$cl ($\Delta\alpha$sc) (%)	−15.4 (2.3)	−22 (1.73)
	ΔCTP (mb)	−141	−8.4

simulation of the strong observed seasonal cycle in low cloud cover exhibited over the Northern Hemisphere ocean areas [*Klein and Hartmann*, 1993]. Also, the GISS model's underprediction of cloud top heights in the large-scale ascent regime is more pronounced in January than in the other three months.

4. Discussion

[18] The evaluation of midlatitude cloud properties in a climate and a weather model revealed several common features between the two models. Those are the overestimation of cloud optical depth in all dynamic regimes, the underestimation of cloud cover in the large-scale descent regime, and the underestimation of cloud top height in the large-scale descent regime. The GISS GCM also underpredicted the amount of high cloud in the large-scale ascent regime, and that resulted in an underprediction by the model of the cloud cover and height in that regime. The analysis of runs with different resolutions revealed large improvement when going from a $4° \times 5°$ 9-layer to a $2° \times 2.5°$ 32-layer run with the GISS GCM, much of which is caused by the increase in vertical resolution. A comparison of a T42 and a T106 run of the same vertical resolution with the ECMWF GCM did not show considerable differences between the two model versions.

[19] The comparison of the forecast and "climate" runs of the ECMWF model showed remarkable similarities in the statistical properties of the clouds. This implies that, for large statistical ensembles, climatological dynamic conditions are sufficient to reproduce the properties of the midlatitude cloud field. This opens the way for the use of weather models in the evaluation of climatological atmospheric fields. Weather models utilize extensively tested dynamics packages and it can be argued that they provide the best possible representation of the atmospheric dynamics. Their use in evaluation studies, then, makes it possible to examine clouds, radiation and a number of other atmospheric fields in the context of relatively "realistic" dynamical forcing. In this study, when runs of similar resolutions of the climate and weather models are compared ($2° \times 2.5°$ 32-layer and T42 31-layer runs in Table 1), the one cloud feature that is consistently better simulated in the weather model run is the amount of high cloud in the large-scale ascent regime. The GISS climate model underestimates the high cloud amount, and this produces model underestimation of both the total cloud cover and the cloud top height in this regime. In all other aspects, the two models show similar deviations from the satellite observations. This means that the underprediction of midlatitude high cloud amount in the GISS GCM that produces significant longwave radiation errors in the model [*Del Genio et al.*, 1996], may be due more to deficiencies in the model large-scale transport of moisture in the midlatitude upper troposphere than to problems in the model cloud scheme. It may also, however, signify problems with the model treatment of ice cloud processes. Increases in vertical resolution improve the simulation of midlatitude high cloud in the GISS model, but even with 53 vertical layers the model high cloud amount is 10% smaller than the ISCCP retrievals. More detailed comparisons of the dynamical transport processes of the two models will be performed to provide better information

on potential deficiencies in the way the GISS GCM transports moisture into the midlatitude regions.

[20] The overprediction by the models of midlatitude cloud optical depth has also been observed in studies with other models [*Norris and Weaver*, 2001; *Webb et al.*, 2001]. In this study, we show that the models tend to compensate for this deficiency in the radiative balance calculations through an underprediction of cloud cover, particularly in the large-scale descent regime. A similar conclusion was reached by *Norris and Weaver* [2001], who found that the NCAR CCM3 overpredicts cloud forcing in large-scale ascent regimes and underpredicts cloud forcing in large-scale descent regimes over the summertime North Pacific. The combination of too large optical thickness and too low cloud cover might lead to a realistic looking simulation of the radiative fluxes at the top of the atmosphere when averaged over a long time period, and might lead to the erroneous conclusion that a model is performing well. *Webb et al.* [2000] also show that the correct top-of-the-atmosphere (TOA) radiative budget can be obtained by a model through compensating errors in the contribution of low-, middle-, and high-top clouds. All this highlights the importance of validating model radiation fields by examining cloud and radiation property changes over the spectrum of dynamic and thermodynamic regimes and not simply by using spatially and temporally averaged cloud and radiation fields.

[21] Comparisons of high-resolution limited-area model runs with radar retrievals done as part of a GCSS WG3 analysis of a North Atlantic storm (P. Clark, personal communication, 2001) show that the models produce excess amounts of column water in the storm region. This is in agreement with the global models' overprediction of cloud optical depth in large-scale ascent regimes presented in this paper. The limited area models overpredict column water both because they produce excessive amounts of water and ice content in each layer and because they tend to fill the whole column with cloud layers in regions of large-scale ascent; radar retrievals along the frontal zone done during the field experiment found smaller overall values of layer liquid and ice content than the models and, on occasion, the presence of dry, cloud-free layers dispersed within the cloudy column. This implies that even high resolution models may not resolve completely dry air intrusions into regions of large-scale ascent and may not simulate correctly in their cloud water calculations the effects of water depleting processes like entrainment and precipitation that reduce cloud water content. All this is the subject of ongoing research efforts in GCSS WG3 that involves the use of limited area and global models as well as satellite and field study observations.

[22] The underprediction by the models of cloud cover in the large-scale descent regime is an issue that relates to the well known difficulties that models have to correctly predict marine stratocumulus decks over oceans [e.g., *Del Genio et al.*, 1996; *Norris and Weaver*, 2001]. This study shows that similar problems exist to an even larger degree over continental regions, where models severely underpredict the amounts of low clouds especially in calm (descending air) large-scale conditions. It is also shown that for the two models used here, an increase in horizontal resolution does not improve the simulation of these types of cloud (Table 1). This underlines once more the well-known difficulties in

simulating boundary layer clouds, a still unsolved problem in large-scale cloud modeling.

[23] As cloud processes in the midlatitude regions are, to a large extent, governed by atmospheric dynamics, significant cloud feedbacks in those regions can result from shifts in the frequency distribution of the different dynamic regimes [*Tselioudis et al.*, 2000]. Such shifts would produce both shortwave and longwave cloud radiative signatures. The fact that models overpredict cloud optical depth in all midlatitude dynamic regimes severely restricts their ability to predict the magnitude of cloud feedbacks. Since cloud albedo is not linearly related to cloud optical depth, small changes in the already excessively large optical depth of the model clouds, even if they are of the right sign and magnitude, would produce smaller radiative signatures than similar changes in smaller, more realistic cloud optical depths. This implies that the models lack sensitivity to potential shortwave cloud feedbacks in the midlatitude regions. This makes it important, then, to evaluate in more detail model simulations of cloud water content and cloud layering in midlatitude locations in order to understand the reasons for the model cloud optical depth deficiencies. Since the first global satellite retrievals of cloud vertical distribution will come from the CLOUDSAT mission and will not be available for the next few years, it is important to utilize local but long-term radar retrievals like the ones provided by the ARM program and near-global radiosonde measurements to resolve cloud layering variations and evaluate global model midlatitude cloud fields.
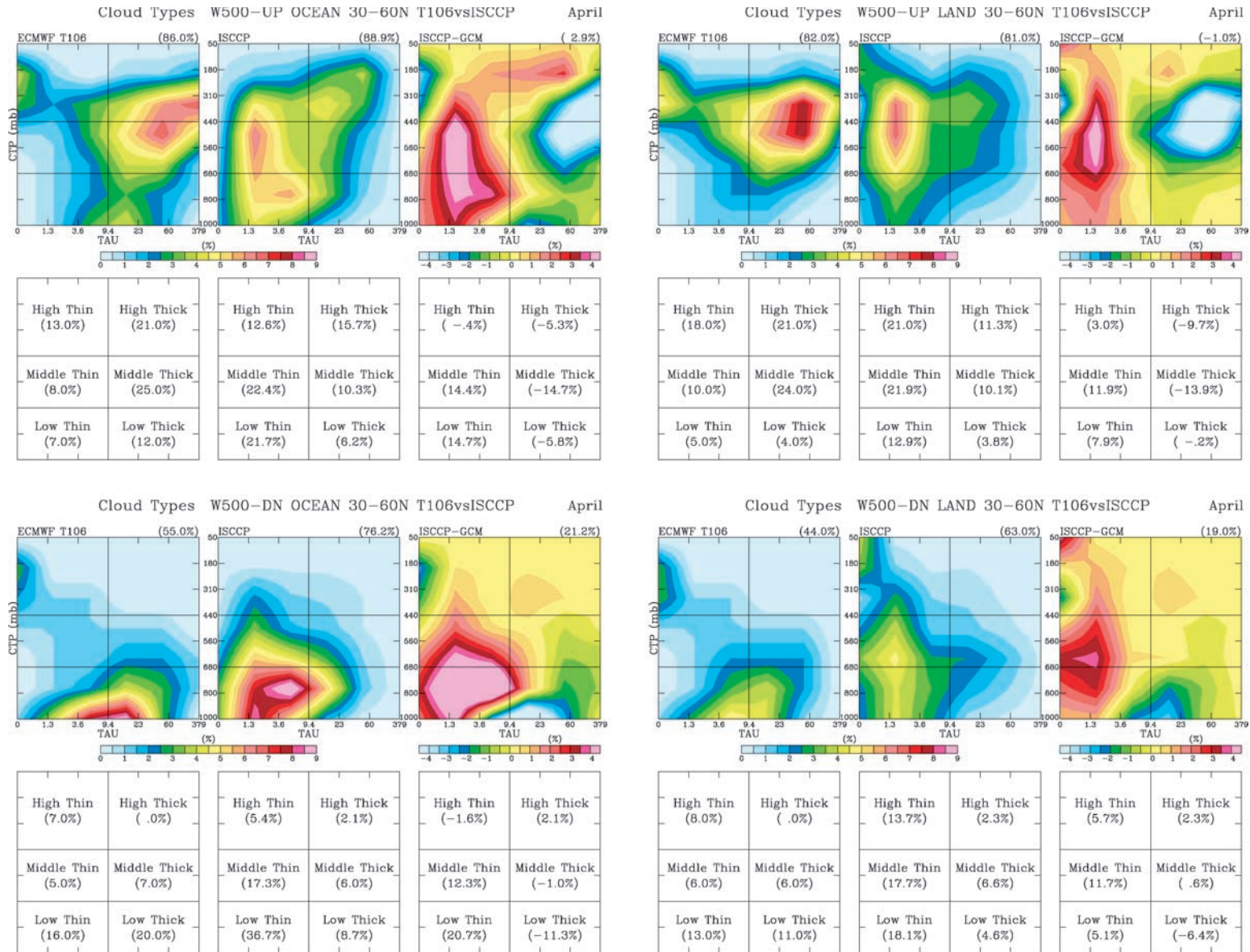
References

Dai, A., A. D. DelGenio, and I. Y. Fung, Implications of observed precipitation and cloud cover changes for diurnal temperature range (DTR), *Nature*, *386*, 665–666, 1997.

Del Genio, A. D., M.-S. Yao, W. Kovari, and K.-W. Lo, A prognostic cloud water parameterization for global climate models, *J. Clim.*, *9*, 270–304, 1996.

Gibson, J. K., P. Kallberg, S. Uppala, A. Hernandez, A. Nomura, E. Serrano, ERA description, ECMWF Re-Analysis Project Report Series, 1, *ECMWF*, Reading, UK, 1997.

Gleckler, P. J., et al., Cloud-radiative effects on implied ocean energy transports as simulated by atmospheric general circulation models, *Geophys. Res. Lett.*, *22*, 791–794, 1995.

Gregory, D., J.-J. Morcrette, C. Jakob, A. C. M. Beljaars, and T. Stockdale, Revision of convection, radiation and cloud schemes in the ECMWF Integrated Forecasting System, *Q. J. R. Meteorol. Soc.*, *126*, 1685–1710, 2000.

Hahmann, A. N., D. M. Ward, and R. E. Dickinson, Land surface temperature and radiative fluxes response of the NCAR CCM2/Biosphere-Atmosphere Transfer Scheme to modifications in the optical properties of clouds, *J. Geophys. Res.*, *100*, 23,239–23,252, 1995.

Hansen, J. E., G. Russell, D. Rind, P. Stone, A. Lacis, S. Lebedeff, R. Ruedy, and L. Travis, Efficient three-dimensional global models for climate studies: Models I and II, *Mon. Weather Rev.*, *111*, 609–662, 1983.

Hansen, J. E., D. Rind, A. DelGenio, A. Lacis, S. Lebedeff, M. Prather, R. Ruedy, T. Karl, Regional greenhouse climate effects, in *Coping with Climate Change*, pp. 68–81, Clim. Inst., Washington, D.C., 1989.

Jakob, C., and S. A. Klein, The role of vertically varying cloud fraction in the parametrization of microphysical processes in the ECMWF model, *Q. J. R. Meteorol. Soc., Part A*, *125*(555), 941–965, 1999.

Klein, S. A., and D. L. Hartmann, The seasonal cycle of low stratiform clouds, *J. Clim.*, *6*(8), 1587–1606, 1993.

Klein, S. A., and C. Jakob, Validation and sensitivities of frontal clouds simulated by the ECMWF model, *Mon. Weather Rev.*, *127*, 2514–2531, 1999.

Lau, N.-C., and M. W. Crane, A satellite view of the synoptic scale organization of cloud properties in midlatitude and tropical circulation systems, *Mon. Weather Rev.*, *123*, 1984–2006, 1995.

Lau, N.-C., and M. W. Crane, Comparing satellite and surface observations of cloud patterns in synoptic-scale circulation systems, *Mon. Weather Rev.*, *125*, 3172–3189, 1997.

Morcrette, J. J., and C. Jakob, The response of the ECMWF model to changes in the cloud overlap assumption, *Mon. Weather Rev.*, *128*, 1707–1732, 2000.

Norris, J. R., and C. P. Weaver, Improved techniques for evaluating GCM cloudiness applied to the NCAR CCM3, *J. Clim.*, *14*, 2540–2550, 2001.

Rossow, W. B., and R. A. Schiffer, Advances in understanding clouds from ISCCP, *Bull. Am. Meteorol. Soc.*, *80*, 2261–2288, 1999.

Rossow, W. B., A. W. Walker, D. E. Beuschel, M. D. Roiter, International Satellite Cloud Climatology Project (ISCCP) Documentation of New Cloud Data Sets, WMO/TD 737, World Climate Research Programme, Geneva, Switzerland, 1996.

Ryan, B. F., J. J. Katzfey, D. J. Abbs, C. Jakob, U. Lohmann, B. Rockel, L. D. Rotstayn, R. E. Stewart, K. K. Szeto, G. Tselioudis, and M. K. Yau, Simulations of a cold front by cloud-resolving, limited-area and large-scale models and a model evaluation using in-situ and satellite observations, *Mon. Weather Rev.*, *128*, 3218–3235, 2000.

Tselioudis, G., Y.-C. Zhang, and W. B. Rossow, Cloud and radiation variations associated with Northern midlatitude low and high sea level pressure regimes, *J. Clim.*, *13*, 312–327, 2000.

Weaver, C. P., and V. Ramanathan, The link between summertime cloud radiative forcing and extratropical cyclones in the North Pacific, *J. Clim.*, *9*, 2093–2109, 1996.

Weaver, C. P., and V. Ramanathan, Relationships between large-scale vertical velocity, static stability, and cloud radiative forcing over Northern Hemisphere extratropical oceans, *J. Clim.*, *10*, 2871–2887, 1997.

Webb, M., C. Senior, S. Bony, and J.-J. Morcrette, Combining ERBE and ISCCP data to assas clouds in the Hadley Centre, ECMWF and LMD atmospheric climate models, *Clim. Dyn.*, *17*, 905–922, 2001.

─────────────────

C. Jakob, Bureau of Meteorology Research Centre, 150 Lonsdale Street, GPO Box 1289K, Melbourne, VIC 3001 Australia. (c.jakob@bom.gov.au)

G. Tselioudis, NASA/GISS, Columbia University, 2880 Broadway, New York, NY 10025, USA. (gtselioudis@giss.nasa.gov)
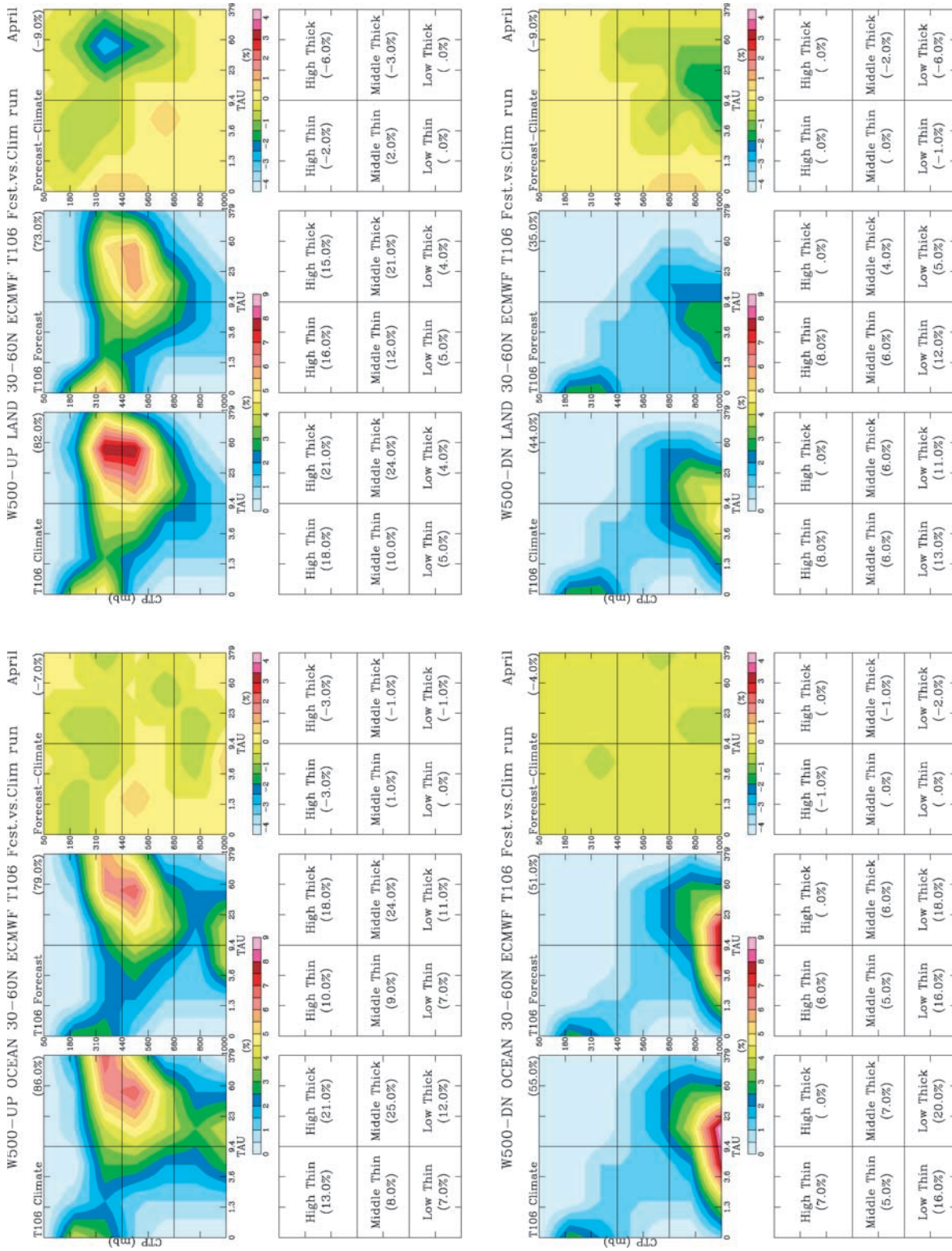
Figure 2. Top two panels represent the large-scale ascent and the bottom two panels the large-scale descent regime, and the left two panels show clouds over ocean and the right two panels clouds over land. Each panel includes cloud optical thickness-cloud top pressure histograms (top row) and tables with cloud cover values in six broad cloud categories (bottom row), for the ECMWF T106 climate run (left column) forecast run (middle column) and the difference between the two (right column). The total cloud cover is noted in parenthesis at the top of each cloud property histogram.

Figure 3. Top two panels represent the large-scale ascent and the bottom two panels the large-scale descent regime, and the left two panels show clouds over ocean and the right two panels clouds over land. Each panel includes cloud optical thickness-cloud top pressure histograms (top row) and tables with cloud cover values in six broad cloud categories (bottom row), for the ECMWF T106 climate run (left column) ISCCP retrievals (middle column) and the difference between the two (right column). The total cloud cover is noted in parenthesis at the top of each cloud property histogram.
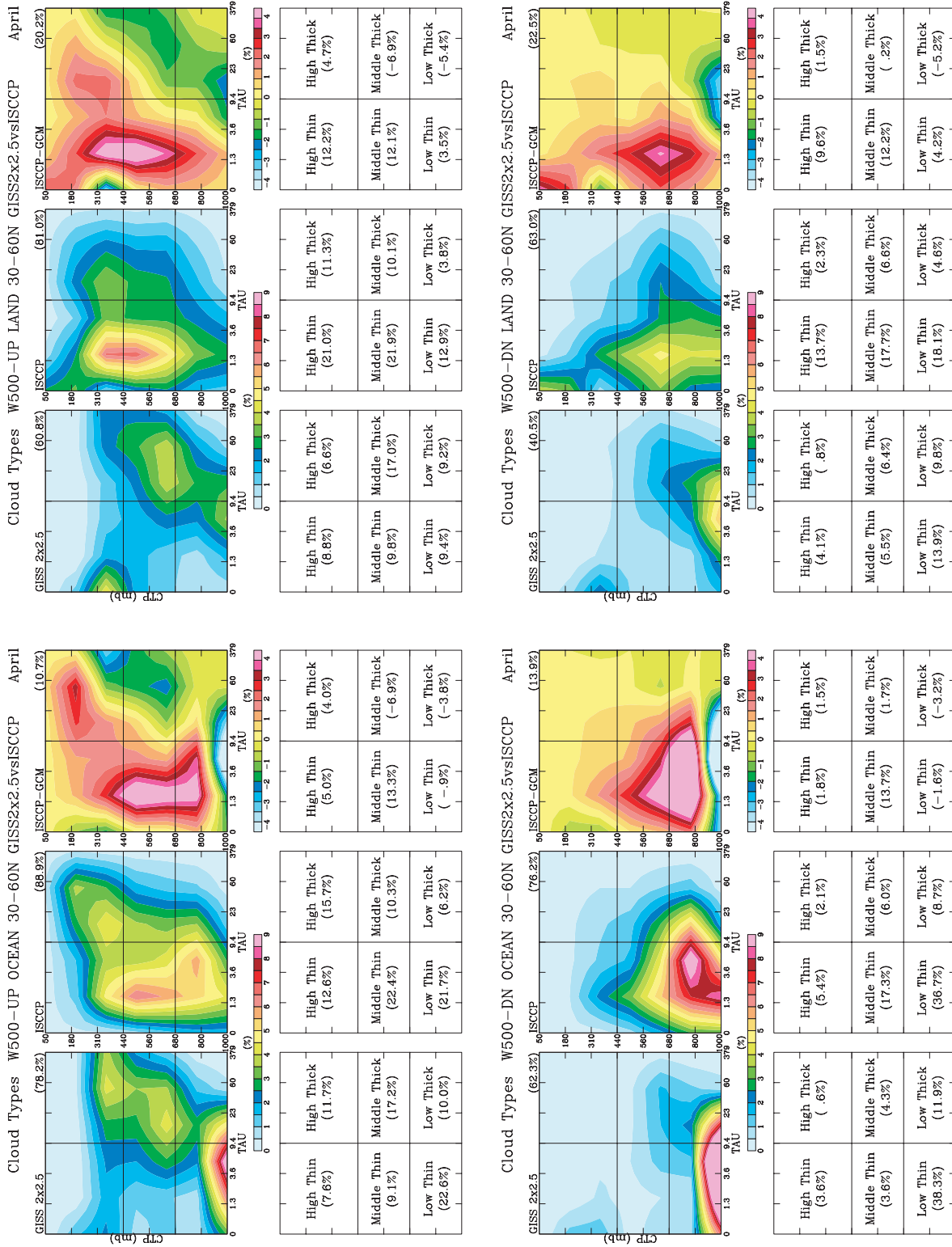
Figure 4. As in Figure 3 for the GISS 2° × 2.5° 32-layer model.